

# Antcin B and Its Ester Derivative from *Antrodia camphorata* Induce Apoptosis in Hepatocellular Carcinoma Cells Involves Enhancing Oxidative Stress Coincident with Activation of Intrinsic and Extrinsic Apoptotic Pathway

Yun-Chih Hsieh,<sup>†</sup> Yerra Koteswara Rao,<sup>‡</sup> Jacqueline Whang-Peng,<sup>§</sup> Chi-Ying F. Huang,<sup>||</sup> Song-Kun Shyu,<sup>⊥</sup> Shih-Lan Hsu,<sup>\*,†</sup> and Yew-Min Tzeng<sup>\*,‡</sup>

<sup>†</sup>Department of Education and Research, Taichung Veterans General Hospital, Taichung 40705, Taiwan, ROC

<sup>‡</sup>Institute of Biochemical Sciences and Technology, Chaoyang University of Technology, Taichung 41349, Taiwan, ROC

<sup>§</sup>Cancer Center, Wan Fang Hospital, Taipei Medical University, Taipei 11601, Taiwan, ROC

<sup>||</sup>Institute of Clinical Medicine, National Yang-Ming University, Taipei 11206, Taiwan, ROC

<sup>⊥</sup>Institute of Biomedical Sciences, Academia Sinica, Taipei 11503, Taiwan, ROC

 Supporting Information

**ABSTRACT:** The triterpenoids methylantcin B (MAB) and antcin B (AB), isolated from the medicinal mushroom *Antrodia camphorata*, have been identified as strong cytotoxic agents against various type of cancer cells; however, the mechanisms of MAB- and AB-induced cytotoxicity have not been adequately explored. This study investigated the roles of caspase cascades, reactive oxygen species (ROS), DNA damage, mitochondrial disruption, and Bax and Bcl-2 proteins in MAB- and AB-induced apoptosis of hepatocellular carcinoma (HCC) HepG2 cells. Here, we showed that MAB and AB induced apoptosis in HepG2 cells, as characterized by increased DNA fragmentation, cleavage of PARP, sub-G1 population, chromatin condensation, loss of mitochondrial membrane potential, and release of cytochrome *c*. Increasing the levels of caspase-2, -3, -8, and -9 activities was involved in MAB- and AB-induced apoptosis, and they could be attenuated by inhibitors of specific caspases, indicating that MAB and AB triggered the caspase-dependent apoptotic pathway. Additionally, the enhanced apoptotic effect correlates with high expression of Fas, Fas ligand, as well as Bax and decreased protein levels of Bcl-X<sub>L</sub> and Bcl-2, suggesting that both the extrinsic and intrinsic apoptosis pathways were involved in the apoptotic processes. Incubation of HepG2 cells with antioxidant enzymes superoxide dismutase and catalase and antioxidants *N*-acetylcysteine and ascorbic acid attenuated the ROS generation and apoptosis induced by MAB and AB, which indicate that ROS plays a pivotal role in cell death. NADPH oxidase activation was observed in MAB- and AB-stimulated HepG2 cells; however, inhibition of such activation by diphenylamine significantly blocked MAB- and AB-induced ROS production and increased cell viability. Taken together, our results provide the first evidence that triterpenoids MAB and AB induced a NADPH oxidase-provoked oxidative stress and extrinsic and intrinsic apoptosis as a critical mechanism of cause cell death in HCC cells.

**KEYWORDS:** methylantcin B, antcin B, hepatocellular carcinoma cells, oxidative stress, extrinsic and intrinsic apoptosis

## INTRODUCTION

Mushrooms have been used in Asia as traditional foods and medicines for a long time, with relative little knowledge of their modes of action.<sup>1</sup> There are various classes of primary and secondary metabolites in mushrooms, and they exhibit significant therapeutic activities.<sup>1</sup> *Antrodia camphorata* (Polyporaceae), popularly known as Niuchangchih in Taiwan, is a well-known medicinal mushroom. Its multiple pharmacological activities on crude extracts include hepatoprotective properties that have been mentioned and summarized.<sup>2–4</sup> For example, it has been reported that methanol extracts from mycelia of *A. camphorata* induce apoptosis in HepG2 cells;<sup>5–7</sup> however, the precise compound and their molecular mechanisms responsible for the observed activity is not known. The major bioactive compounds of *A. camphorata* are triterpenoids, steroids, benzenoids, maleic/succinic acid derivatives, and polysaccharides.<sup>2</sup> Some of our preliminary studies have indicated that triterpenoids,

methylantcin B (MAB) and antcin B (AB), from *A. camphorata* show selective cytotoxicity against a variety of tumor cells, with a higher activity than that shown against normal cells.<sup>8</sup> MAB and AB also induce mitochondria-mediated apoptosis in human colon cancer HT-29 cells.<sup>8</sup> However, there is no study addressing the detailed apoptosis mechanism induced by MAB and AB in human hepatocellular carcinoma (HCC) cells. In the course of our search for beneficial therapeutic compounds from *A. camphorata*,<sup>8–12</sup> the cytotoxic effect of these triterpenoids started to draw attention. Therefore, we propose to examine on HCC cells, the apoptotic activities of MAB and AB as well as to

**Received:** July 14, 2011

**Accepted:** September 14, 2011

**Revised:** September 5, 2011

**Published:** September 14, 2011

elucidate the role of reactive oxygen species (ROS) in the apoptotic activity of these promising bioactive compounds.

Apoptosis or programmed cell death is essential for maintenance of development and homeostasis of multicellular organisms by eliminating superfluous or unwanted cells. Deregulation of apoptosis is the hallmark of all cancer cells, and the agents that activate apoptosis in cancer cells could be valuable anticancer therapeutics.<sup>13</sup> Apoptosis is characterized by the activation of the caspases family of cysteine proteases, followed by caspase-mediated specific morphological changes, including unclear DNA fragmentation.<sup>13</sup> Recent studies have provided ample evidence that two major pathways including intrinsic and extrinsic apoptotic signaling are involved in the regulation of apoptosis.<sup>14</sup> The extrinsic apoptotic pathway involves cell surface death receptors, such as Fas/CD95 and TNFR1, which, upon activation, up-regulate the downstream signaling cascade leading to the activation of caspase-8. The intrinsic pathway involves the cell oxidative stress that triggers the mitochondria-dependent pathway, resulting in the induction of decreased mitochondrial membrane potential, altered ratio of Bcl-2 family members affecting cytochrome *c* release from mitochondria into cytosol, and the activation of caspase cascade.<sup>14</sup>

ROS, a group of highly reactive molecules, have been shown to play a key role in apoptotic cell death.<sup>15</sup> Mitochondria are known to be one of the major generators of ROS in cells. Dysfunction of electron transfer through the mitochondrial respiratory chain may result in increased ROS formation.<sup>15</sup> ROS can oxidize a wide range of cell constituents, including lipids, proteins, and DNA, thus damaging cell structures and compromising function. When antioxidant mechanisms are overwhelmed by ROS and subsequent oxidative stress occurs, cell damage and cell death are induced.<sup>15</sup> Often, the ability of a therapeutic agent to induce apoptosis of cancer cells depends upon the ability of cancer cells to generate ROS.<sup>16</sup> The involvement of ROS in the induction of apoptosis of a variety of cancer cells has been widely reported.<sup>15–18</sup> Therefore, we investigated the role of ROS in the MAB- and AB-induced apoptosis in HCC cells. Our results presented here suggest that enhanced oxidative stress and a change in the expression pattern of apoptosis-related proteins might be responsible for MAB- and AB-induced apoptosis.

## MATERIALS AND METHODS

**Chemicals and Reagents.** Propidium iodide (PI), dimethyl sulfoxide (DMSO), 3-(4,5-dimethylthiazol-2-yl)-2,5-diphenyltetrazolium bromide (MTT), ribonuclease (RNase), diphenylamine (DPI), lucigenin, superoxide dismutase (SOD), catalase (CAT), ascorbic acid (ASC), and *N*-acetylcysteine (NAC) were purchased from Sigma-Aldrich (St. Louis, MO). 2',7'-Dichlorofluorescein diacetate (DCFH-DA), and dihydroethidine (HE) were purchased from Molecular Probes (Eugene, OR). Fetal calf serum (FCS) and Dulbecco's modified Eagle's medium (DMEM) were purchased from GIBCO BRL (Gaithersburg, MD). Anti-tubulin, -Bcl2, -Fas (C-20), -Bcl<sub>XL</sub>, and -Bax antibodies were purchased from Santa Cruz Biotechnology (Santa Cruz, CA). Anti-Fas (clone ZB4) antagonistic antibody was purchased from Upstate Biotechnology (Lake Placid, NY). Anti-cytochrome *c* antibody was purchased from PharMingen (San Diego, CA). Anti-actin antibody was purchased from Oncogene Science Inc. (Uniondata, NY). Caspase activity assay kits were purchased from R&D Systems (Minneapolis, MN). Caspase-2 inhibitor (Z-VDVAD-FMK), caspase-3 inhibitor (Z-DEVD-FMK), caspase-8 inhibitor (Z-IETD-FMK), and caspase-9 inhibitor

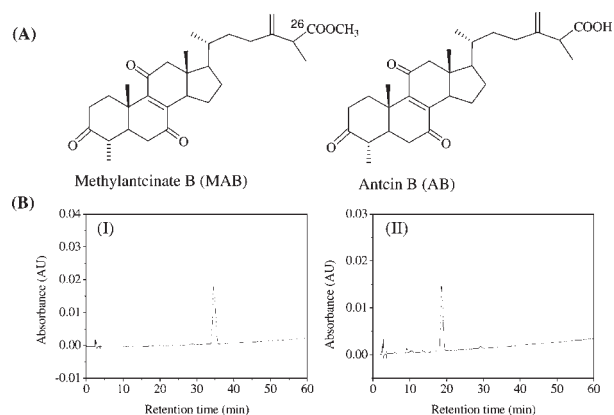


**Figure 1.** (A) Chemical structures of methylantcinate B (MAB) and antcin B (AB). (B) HPLC chromatogram of MAB (I) and AB (II). Chromatographic analysis was performed with a J'sphere ODS-M80 C18 column (250 × 4.6 mm, 4 μm, YMC Co., Ltd.). The mobile phase consisted of CH<sub>3</sub>CN (solvent A) and water containing 0.2% acetic acid (solvent B). A linear gradient program was used as follows: 60% A in the first 0 min, linear gradient to 90% A over 60 min. The injection volume was 5 μL. The mobile phase flow rate was 0.8 mL/min, and the detector was monitored at 268 nm.

(Z-LEHD-FMK) were purchased from KAMIYA (Seattle, WA). Anti-COX IV antibodies were purchased from Cell Signaling Technology (Danvers, MA). TUNEL assay kit was purchased from Roche Diagnostics (Mannheim, Germany). JC-1 (5,5',6,6'-tetrachloro-1,1',3,3'-tetraethylbenzamidazolyl carbocyanine iodide) was purchased from Biovision (Mountain View, CA). Adenovirus Bcl-2 was kindly provided by Dr. Song-Kun Shyue of the Institute of Biomedical Science of Academia Sinica (Taipei, Taiwan).

**Extraction and Isolation of Triterpenoids MAB and AB.** The fruiting bodies of *A. camphorata* were collected from the Yuli, Hualien County, Taiwan, in December 2007. The species was identified by Prof. Yew-Min Tzeng at Natural Products & Bioprocess Laboratory, Chaoyang University of Technology. A voucher specimen (YMT 7002) was deposited in the Herbarium of the Institute of Biochemical Sciences and Technology, Chaoyang University of Technology, Taiwan, ROC.

The compounds MAB and AB (Figure 1A) were purified and identified from the fruiting bodies of *A. camphorata* following the reported extraction and isolation procedures.<sup>8</sup> Briefly, the air-dried powder of the fruiting bodies was successively extracted with *n*-hexane, chloroform, and methanol under reflux. After exhaustive extraction, the combined extracts were concentrated individually under reduced pressure. The CHCl<sub>3</sub> soluble fraction was chromatographed over silica gel using *n*-hexane/EtOAc gradient eluent, and similar fractions were combined to produce five fractions (A–E). Fractions B and C were further separated using a silica gel column eluting with a gradient of *n*-hexane/EtOAc to afford MAB and AB, respectively. The structures of MAB and AB were determined on the basis of the proton and carbon signals (Supporting Information, Figures S1–S6), which appeared with almost the same chemical shifts and identical multiplicity as established previously.<sup>8</sup> The purity (>95%) of MAB and AB were confirmed by an HPLC [J'sphere ODS-M80 C18 column, 250 × 4.6 mm, 4 μm (YMC Co., Ltd.)]. The mobile phase consisted of acetonitrile (solvent A) and water containing 0.2% acetic acid (solvent B). A linear gradient program was used as follows: 60% A in the first 0 min, linear gradient to 90% A over 60 min. The injection volume was 5 μL. The mobile phase flow rate was 0.8 mL/min, and the detector was monitored at 268 nm. Representative HPLC chromatograms are shown in Figure 1B.

**Cell Culture and Cytotoxicity.** Human hepatocellular carcinoma HepG2, Hep3B, and Huh7 cell lines were obtained from the American Type Cell Culture Collection (ATCC, Manassas, VA). The cells were cultured in DMEM medium containing 10% FCS, antibiotics (100 U/mL penicillin and 100 U/mL streptomycin), and 2 mM glutamine, at 37 °C in a humidified atmosphere with 5% CO<sub>2</sub>. The rat hepatocytes were isolated through collagenase perfusion from 250–350 g Sprague–Dawley rats and cultured in 12-well plates in DMEM supplemented with 2% fetal bovine serum (FBS).<sup>11</sup> For cytotoxicity assay, cells were treated with various concentrations of MAB or AB for the indicated time point. After treatment, the viable cells were evaluated by MTT assay with a spectrophotometer at 570 nm.<sup>19</sup> Each concentration was repeated three times.

**DNA Fragmentation Analysis.** Cells were treated with DMSO alone and 100 μM of MAB or AB for each time period, and then cells were collected and lysed by DNA extraction buffer (50 mM Tris, pH 7.5, 10 mM EDTA, and 0.3% Triton X-100). The solution was incubated with 0.1 mg/mL proteinase K and 0.2 mg/mL RNase for 1 h, at 55 °C, extracted with phenol–chloroform (1:1), and separate in 2% agarose gel, and then the fragmented DNA was visualized with ethidium bromide and photographed with a UV gel image system.<sup>11</sup>

**Single-Cell Gel Electrophoresis, Comet Assay.** The alkaline comet assay was performed by seeding  $1 \times 10^5$  cells per well into 6-well plastic dishes. After 24 h incubation, cells were treated with 100 μM MAB or AB for an additional 24 h. After treatment, the cells were washed twice with PBS, trypsinized, and analyzed on multispot prototype comet slides (1% agar below the 1.5% low melting agar mix with cells). The slides were kept in a cold fresh lysis buffer (2.5 M NaCl, 100 mM Na<sub>2</sub>EDTA, 10 mM Tris, 1% N-lauroylsarcosine, 1% Triton-X100, 10% DMSO) for 1 h. After lysis, electrophoresis (23 V, 300 mA) was carried out for 25 min under electrophoretic conditions. After neutralization, the slides with the comets equally spread in dried gels were stained for 30 min with ethyl bromide stain (Sigma) in a 1:10 000 dilution in water and dried again at room temperature. Microscopic analysis (Olympus IX81) was conducted using Image Pro Plus for image analysis and statistics. The tail length (measured from the middle of the head to the end of the tail) and the tail moment (tail length × relative tail DNA content) were measured as parameters.

**Apoptotic Cell Determination.** Apoptotic cells were measured by a terminal deoxynucleotidyl transferase dUTP nicked-end labeling (TUNEL) assay by flow cytometry. TUNEL assay was performed according to the manufacturer's instructions (Boehringer Mannheim). PI staining and flow cytometry were used to determine the cell cycle stage and sub-G1 group. Briefly, 100 μM MAB- or AB-treated cells were washed with PBS and fixed with 70% ethanol with gentle vortexing. Fixed cells were spun down and washed with PBS twice, and then cells were permeabilized with 0.1% Triton X-100 in 100 μL of 0.1% sodium citrate for 2 min in ice. After washing two times, the labeling reaction was performed by incubating cells in 50 μL of labeling solution containing the TdT enzyme for 1 h at 37 °C in the dark. Next, cells were resuspended in 500 μL of PI (2 μg/mL)/Triton X-100 (0.1% v/v) staining solution with 100 μg/mL RNase for 30 min in the dark and analyzed by a FACScan flow cytometer. The percentage of apoptotic cells (subG1 population or TUNEL positive fraction) was analyzed using Cell Quest software.

**Caspase Activity Assay.** Cell lysates obtained from MAB-, AB-, or vehicle-treated cells were tested for caspase-2, -3, -8, and -9 activities by addition of caspase-specific peptide substrate conjugated with the fluorescent reporter molecule, according to the manufacturer's instructions (R&D systems Minneapolis, MN). An equal amount of protein from each sample was used to determine the level of caspase enzymatic activity, which is directly proportional to the fluorescence signal detected with a fluorescent microplate reader (Fluoroskan Ascent; Labsystem,

Finland). The relative caspase activity was absorbance excited by light at 400 nm and emitted fluorescence at 505 nm.

**Subcellular Fractionation.** Cells were washed, harvested, and then incubated on ice for 30 min in sucrose buffer (250 mM sucrose, 2 mM EDTA, 2 mM EGTA, 10 mM DTT). Lysates were centrifuged at 1300g for 10 min at 4 °C, and the soluble cytosolic fraction was collected after further centrifugation of the raw cytosolic fraction at 1300g for 30 min at 4 °C. Mitochondria were purified from heavy membrane fraction by sucrose density-gradient centrifugation; briefly, the heavy membrane pellet was resuspended in 1 mL of sucrose buffer and laid on the top of a 1.2 and 1.5 M sucrose buffer gradient before being centrifuged at 1300g for 30 min at 4 °C. Sucrose-density-gradient-purified mitochondria-enriched fractions were collected at 1.2/1.5 M interphases, respectively, washed with PBS, and dissolved in RIPA lysis buffer. All fractions were disrupted by sonication and prepared before Western blot analysis.

**Protein Preparation and Immunoblotting.** Cells were cultured without or with 100 μM MAB or AB at indicated times. After treatment, cells were harvested, washed twice with ice-cold PBS, and lysed in modified RIPA buffer with protease inhibitors. The cell lysates were cleared by centrifugation at 12 000g for 30 min at 4 °C, the total protein content of the supernatant was collected and determined by the Bradford method. For Western blot analysis, equal amounts of total protein were loaded onto SDS–polyacrylamide gels, and the proteins were electrophoretically transferred onto a PVDF membrane (Millipore, Bedford, MA). The protein expression was detected by each immunoblotting with the corresponding specific primary antibodies (against PARP, Bcl-X<sub>L</sub>, Bcl-2, Bax, actin, cytochrome c, COX IV, and tubulin) at 4 °C for 16 h. After washing three times with TBST, the membrane was incubated with horseradish peroxidase-labeled secondary antibody for 1 h. The membrane was washed, and detection was performed using the enhance chemiluminescence blotting detection system (Amersham).

**Determination of Intracellular Reactive Oxygen Species (ROS) Level and Mitochondrial Membrane Potential ( $\Delta\Psi_m$ ).** To assess the intracellular ROS level, the cells were incubated with 100 μM MAB or AB for the indicated periods. Cells were incubated with 10 μM DCFHDA or 10 μM HE for 30 min prior to harvesting. In the presence of ROS, the DCF-DA will convert to DCFH, which can be oxidized to the fluorescent compound DCF. The fluorescence intensity of the cells was analyzed by flow cytometry. The  $\Delta\Psi_m$  is assessed using a lipophilic fluorochrome (JC-1, Molecular Probes). Briefly, cells were treated with 100 μM MAB or AB for the indicated periods. Before harvested each time points, cells were incubated in medium with JC-1 for 30 min and then washed with PBS. Both red and green fluorescence emissions were analyzed by flow cytometry using an excitation wavelength of 488 nm and observation wavelengths of 530 nm for green fluorescence and 585 nm for red fluorescence.

**NADPH Oxidase Activity Assay.** This assay was performed by following the procedure described previously.<sup>11</sup> The cells were lysed using Dounce homogenizer, and the cell lysate concentration was determined by the Bradford method. Aliquot proteins were added to the reaction buffer (50 mM phosphate buffer pH 7.0, 1 mM EGTA, 150 mM sucrose, and 5 μM lucigenin as the electron acceptor, and 100 μM NADPH as the substrate). The reaction was initiated by the addition of 100 μL/tube protein (50 and 25 μg) and 900 μL reaction buffers, and photon emission was measured every minute for a 15 min time period using a microtiterplate luminometer. The activity was expressed as relative light units (RLU) per minute per milligram of total protein (RLU/min/mg protein).

**Statistical Analyses.** Each experiment was performed in triplicate and repeated three times. The results were expressed as mean ± SEM. Statistical comparisons were made by means of one-way analysis of variance (ANOVA), and significant difference between the tested groups was using Student's *t*-test. The statistic significance was set at \**p* < 0.05, \*\**p* < 0.01, \*\*\**p* < 0.001.

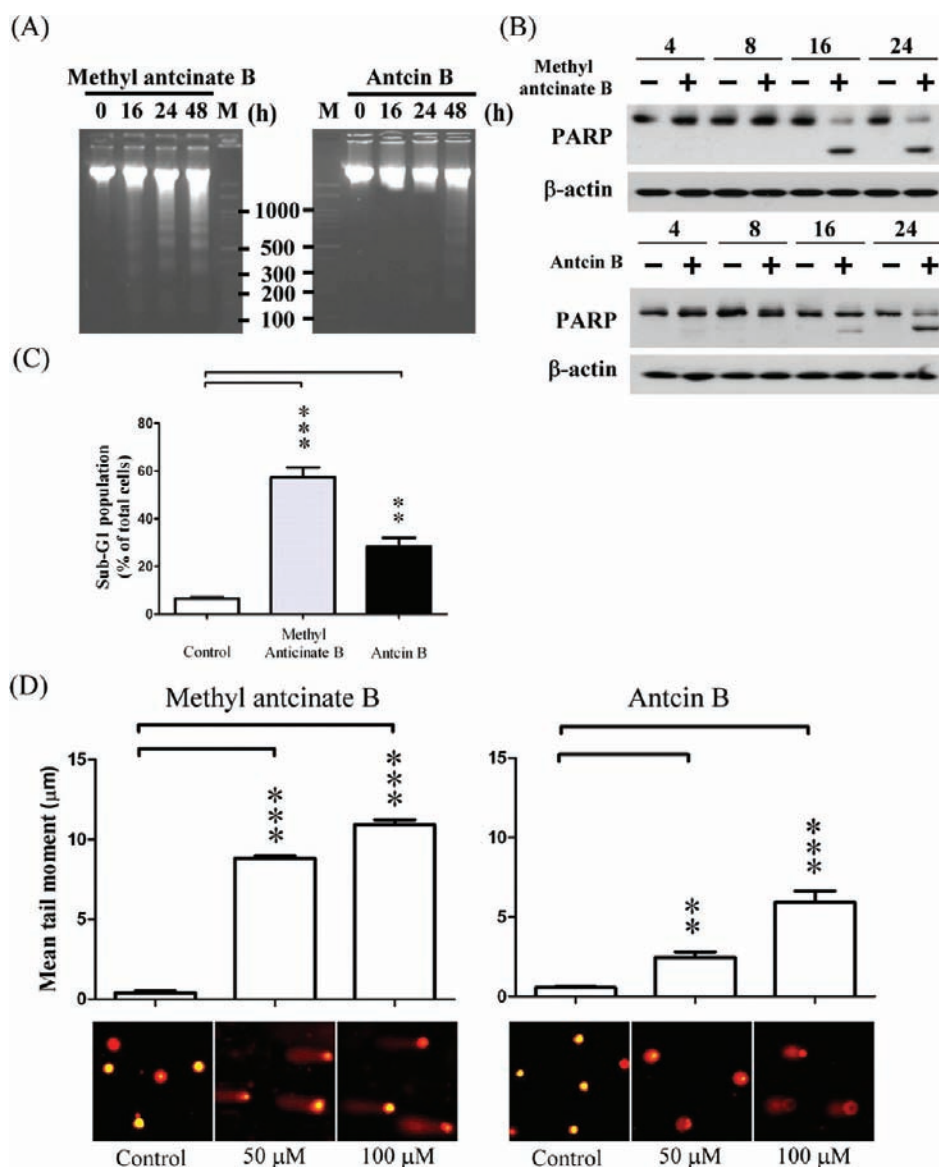


**Figure 2.** Methylandcinate B (MAB) and antcin B (AB) induce DNA fragmentation and apoptosis in HepG2 cells. (A) DNA fragmentation. HepG2 cells were exposed to 100  $\mu\text{M}$  of MAB or AB for indicated times (0, 16, 24, and 48 h), and then genomic DNA was isolated. DNA samples were loaded into 2% agarose gel by electrophoresis. (B) The cleaved PARP was determined by Western blot. (C) Sub-G1 population refers to apoptotic cells. (D) Single cell gel electrophoresis (comet) assay. Twenty-four hours after incubation with 50 or 100  $\mu\text{M}$  MAB or AB, the cells were subjected to alkaline unwinding and electrophoretic conditions, as described in Materials and Methods. Labeled DNA was visualized under a fluorescence microscope. Cells with damaged DNA displayed a comet. Data are presented as mean  $\pm$  SD from three independent experiments. \*\* $p < 0.01$  and \*\*\* $p < 0.001$ , as compared to control DMSO treatment values.

## RESULTS

**MAB- and AB-Induced Apoptosis in HCC Cells.** In a primary screening test, to determine the effect of triterpenoids MAB and AB on cell viability, HCC cell lines HepG2, Hep3B, and Huh7 were treated with one of various concentrations of MAB or AB for 48 h. We found that MAB and AB inhibited HepG2, Hep3B, and Huh7 cell viability as determined by the MTT assay in a dose-dependent manner, and the inhibitory results were in agreement with our previous report.<sup>8</sup> Although, triterpenoids inhibited cell viability, cells were more sensitive to MAB as the resulted  $\text{IC}_{50}$  values were 25.8, 70.3, 29.8  $\mu\text{M}$  for MAB but 39.4, 50.6, 45.3  $\mu\text{M}$  for AB against HepG2, Hep3B and Huh7 cells, respectively. We compared the effects of MAB and AB in

inhibiting cell viability between cancer and noncancer cells, and it was found that the  $\text{IC}_{50}$  of MAB and AB against primary rat hepatocytes derived from normal rat liver was greater than 500  $\mu\text{M}$  (data not shown). These results indicate that MAB and AB were more potent in inhibiting cancer cell viability than noncancer cells. The cell line HepG2, sensitive to the MAB and AB, was chosen to elucidate the molecular events associated with cell viability inhibition.

To investigate whether the observed cell viability inhibition was caused by apoptosis, DNA fragmentation, poly(ADP-ribose) polymerase (PARP) cleavage, and cell cycle analyses were performed. The genomic DNA isolated from HepG2 cells treated with 100  $\mu\text{M}$  of MAB or AB for 16, 24, or 48 h was

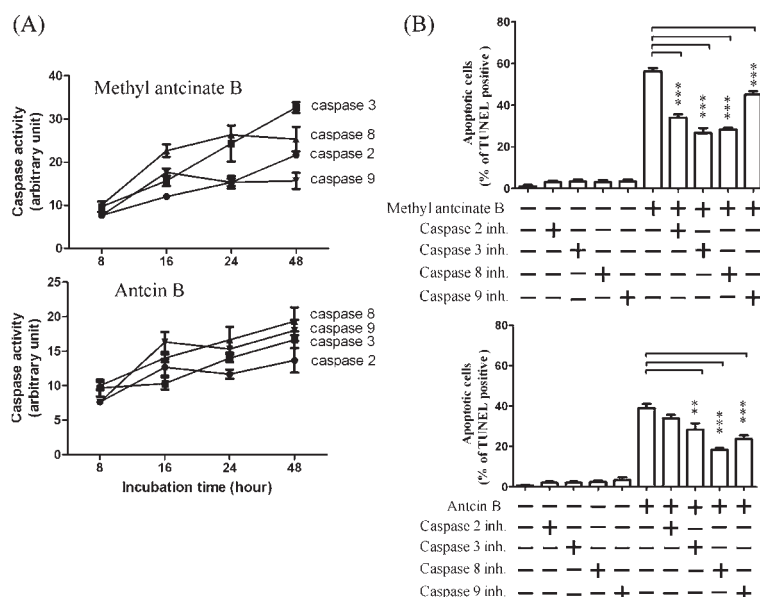


**Figure 3.** Methylantcin B (MAB) and antcin B (AB) induce caspase-dependent apoptosis. (A) Activation of caspases. HepG2 cells were incubated with 100  $\mu$ M MAB or AB for indicated time periods (8, 16, 24, and 48 h), and then cell lysates were extracted, and caspase activity was detected by each specific substrate. (B) Caspase inhibitor blocked MAB- and AB-triggered apoptosis. HepG2 cells were pretreated with 30  $\mu$ M caspase inhibitor for 1 h and incubated with 100  $\mu$ M of MAB or AB for another 24 h. The apoptotic cells were detected by TUNEL/PI assay by flow cytometry. Data are expressed as the mean  $\pm$  SD from three independent experiments. \*\* $p$  < 0.01 and \*\*\* $p$  < 0.001, as compared to control DMSO treatment values.

separated by agarose gel electrophoresis. Again, the effect with AB was smaller than with MAB at the same concentration. As shown in Figure 2A, the internucleosomal DNA fragments were observed after 16 h of MAB treatment and reached a maximum in 48 h, while AB showed such response only after a treatment period of 48 h (Figure 2A). Another apoptotic feature is the appearance of cleaved PARP, which can be determined by Western blot. As shown in Figure 2B, the amount of nuclear full length PARP that was decreased and cleaved into its smaller fragment was significantly increased after 16 and 24 h of MAB and AB treatment (Figure 2B). Flow cytometry assay after propidium iodide staining allows cell cycle analysis, and cells undergoing apoptosis can be detected as a subdiploid peak. The results observed using this technique revealed that 48 h treatment with 100  $\mu$ M MAB or AB elevated the percentage of HepG2 cells in the sub-G1 phase from the control value of 5.43% to 56.5% and 28.9%, respectively (Figure 2C). The comet assay provides a simple and effective method for evaluating DNA damage at the single-cell level. Consistent with apoptosis results, HepG2 cells treated with 50 and 100  $\mu$ M of MAB or AB were found to produce chromatin condensation (an apoptotic characteristic), the effect of MAB being more pronounced (Figure 2D). Taken together, these results suggest that triterpenoids MAB and AB trigger apoptotic cell death in HepG2 cells.

**MAB and AB Increased Caspases Activity.** The activation of the caspase pathway is known to be an important mechanism in apoptotic cell death in most cell systems.<sup>20</sup> To gain further insights into the molecular events associated with MAB- and AB-induced apoptosis, we analyzed caspases-2, -3, -8, and -9 activities in HepG2 cells using a caspase fluorogenic peptide substrate kit. As shown in Figure 3A, upon 100  $\mu$ M of MAB treatment the activities of caspase-3, followed by -8, -2, and -9 were time-dependently increased. On the other hand, under the same experimental conditions, AB increased caspase-8 followed by -9, -3, and -2. To investigate if MAB and AB induced apoptosis

through the caspase cascades dependent pathway, HepG2 cells were individually pretreated with inhibitors of caspase-2 (Z-VDDAD-FMK), caspase-3 (Z-DEVD-FMK), caspase-8 (Z-IETD-FMK), and caspase-9 (Z-LEHD-FMK) before treatment with 100  $\mu$ M MAB or AB for 24 h. Figure 3B showed that these specific inhibitors significantly protected the HepG2 cells from apoptosis, as detected using the TUNEL assay by flow cytometry. These results indicate that the activated caspases might be involved in MAB- and AB-induced apoptosis in HepG2 cells.

**MAB and AB Induced Apoptosis through Extrinsic and Intrinsic Apoptotic Pathway.** To examine the mitochondrial apoptotic events associated with MAB- and AB-induced apoptosis, we examined the levels of pro-apoptotic and anti-apoptotic proteins by Western blot analysis in whole lysates of HepG2 cells treated with 100  $\mu$ M MAB or AB for various periods of time. It was found that MAB or AB treatment increased levels of the pro-apoptotic protein Bax and drastically reduced levels of anti-apoptotic proteins Bcl-2 and Bcl-xL in a time-dependent manner (Figure 4A), indicating the involvement of the intrinsic apoptotic pathway. We then investigated whether Bax was involved in MAB- and AB-related mitochondrial apoptosis. It has been well-documented that during mitochondria-dependent apoptosis, Bax can translocate from cytosol to mitochondrion and form pores to permeabilize the outer membrane of mitochondrion, causing the release of cytochrome *c*.<sup>20</sup> The subcellular localization changes of Bax and cytochrome *c* during MAB- or AB-induced apoptosis were examined by Western blot analysis.  $\alpha$ -Tubulin and Cox IV were used as loading controls for the cytosolic and mitochondrial fractions, respectively. The results in Figure 4B showed that the level of Bax was time-dependently reduced in the cytosol fraction but increased in the mitochondrial part from the HepG2 cells treated with 100  $\mu$ M MAB or AB for 24 h. The ratio of Bax level in cytosol to that in mitochondria decreased from 1.0 to <0.4 at 24 h. The reverse phenomenon was observed for cytochrome *c*, in that its level in the mitochondrial fraction decreased, but the

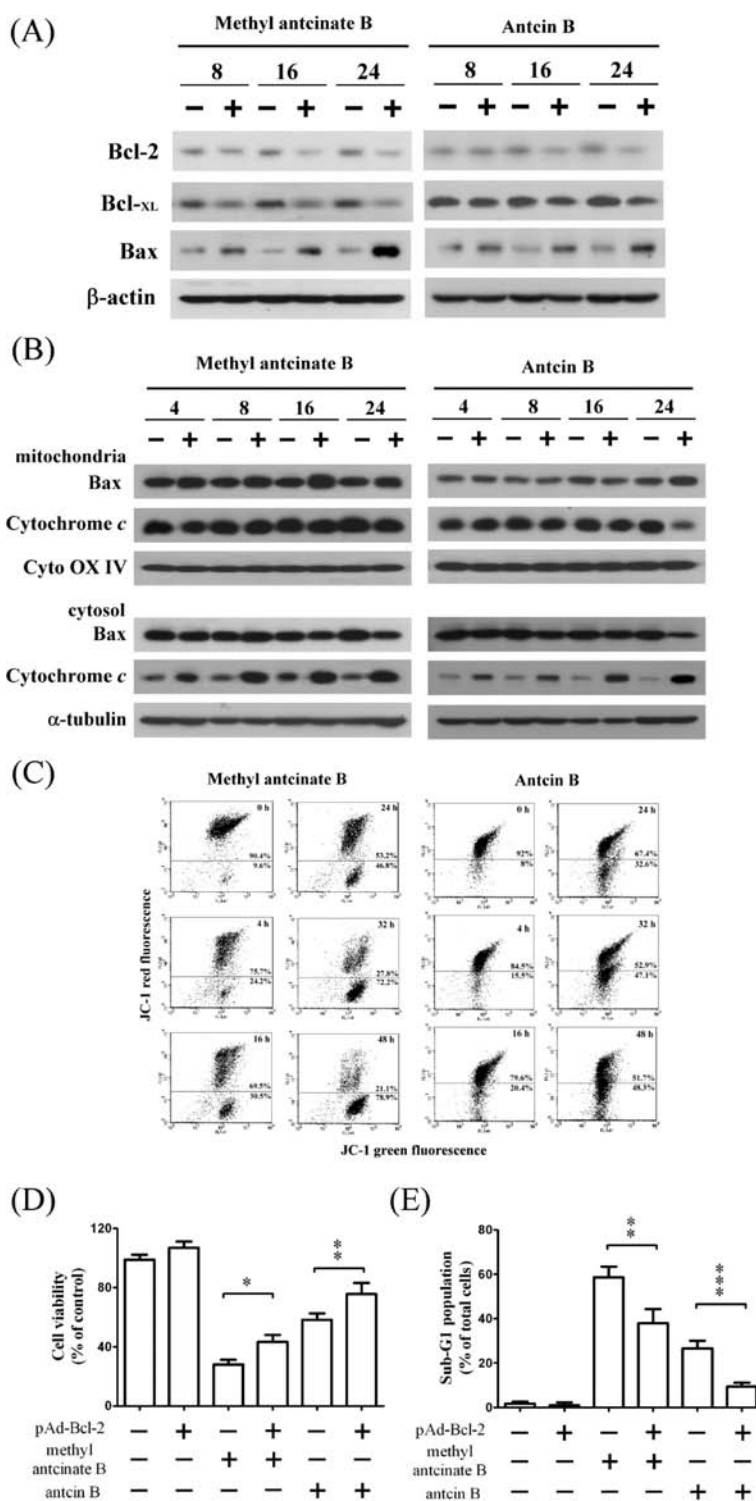


**Figure 4.** Regulation of intrinsic apoptosis-related molecules and alteration of mitochondria membrane potential by methylantcin B (MAB) and antcin B (AB). (A) The protein expression was determined at 8, 16, and 24 h without or with 100  $\mu$ M MAB or AB by Western blot, with  $\beta$ -actin as loading control. (B) Cytochrome *c* localization assay. Cell lysates were isolated from mitochondria and cytosol section from HepG2 cells, and cytochrome *c* and Bax were detected with specific antibody by Western blot. Cyto OX IV and  $\alpha$ -tubulin are internal control of mitochondria and cytosol. (C) Evaluation of mitochondria membrane potential in HepG2 cells was done with JC-1 dye stain by flow cytometry. Distinct populations were detected with 100  $\mu$ M MAB or AB from 0, 4, 16, 24, 32, and 48 h analysis. (D) Cell viability and (E) Sub-G1 population were estimated by trypan blue dye exclusion assay and PI stain FACScan analysis when cells were infected with adenovirus-Bcl2 for 2 days and treated 100  $\mu$ M MAB or AB media for another 24 h. Data are expressed as the mean  $\pm$  SD from three independent experiments. \* $p$  < 0.05, \*\* $p$  < 0.01, and \*\*\* $p$  < 0.001, as compared to control DMSO treatment values.

level in the cytosol increased. The ratio of cytochrome *c* level in cytosol to that in mitochondria increased from 1.0 to 3.5 at

24 h after MAB or AB treatment. These results indicate that MAB and AB can induce apoptosis via a Bax-mediated

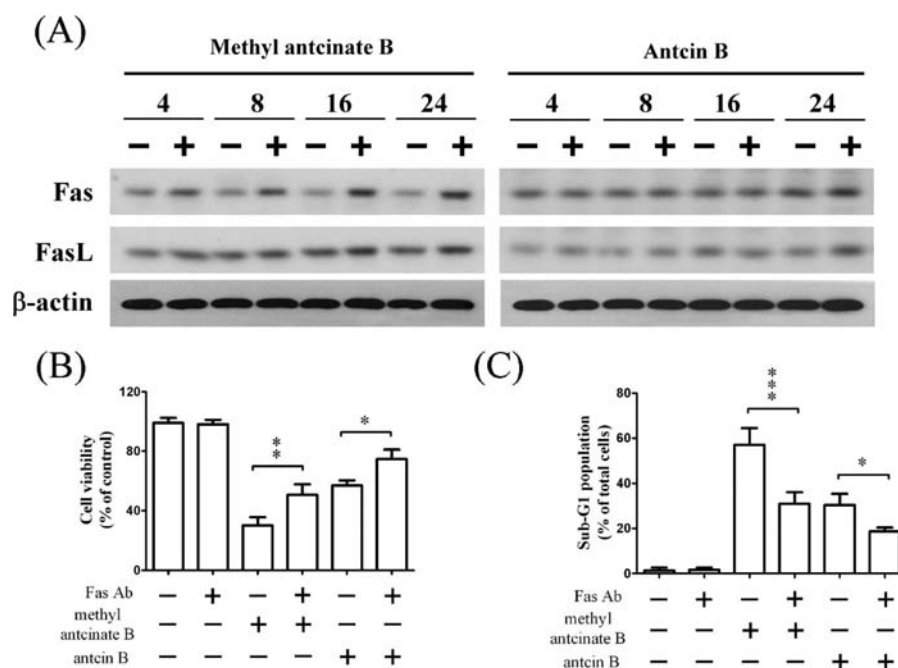


**Figure 5.** Regulation of extrinsic apoptosis-related molecules by methylantcin B (MAB) and antcin B (AB). (A) The protein expression was determined at 4, 8, 16, and 24 h without or with 100  $\mu$ M MAB or AB by Western blot, with  $\beta$ -actin as loading control. (B) Cell viability and (C) Sub-G1 population were estimated by trypan blue dye exclusion assay and PI stain FACScan analysis when cells were exposed with antagonist Fas antibody (2 ng/mL) for 1 h and coincubated 100  $\mu$ M MAB or AB media for another 24 h. Data are presented as mean  $\pm$  SD from three independent experiments. \* $p$  < 0.05, \*\* $p$  < 0.01, and \*\*\* $p$  < 0.001, as compared to control DMSO treatment values.

mitochondria-dependent pathway involving its downstream target cytochrome *c*.

Since the mitochondrial membrane potential is critical in cells undergoing apoptosis, we evaluated whether MAB and AB treatment had any effect on mitochondrial transmembrane potential ( $\Delta\Psi_m$ ). The integrity of the mitochondrial membranes of the cells was examined by JC-1 lipophilic fluorescence staining, and the decrease in JC-1 red fluorescence intensity reflected the loss of  $\Delta\Psi_m$ . The fluorescence intensity of 100  $\mu$ M MAB- or AB-treated cells for the indicated time periods was detected by flow cytometric analysis. As shown in Figure 4C, exposure of HepG2 cells to MAB or AB for 48 h caused a marked loss of  $\Delta\Psi_m$  compared with the control group. In particular, with a treatment period of 4, 16, 24, 32, and 48 h, MAB decreased the percentages of red fluorescence cells from 90.4 to 75.7, 69.5, 53.2, 43.5, and 32.6%, respectively, while AB reduced the same from 92 to 84.5, 79.6, 67.4, 52.9, and 51.7%, respectively (Figure 4C). To further confirm the role of Bcl-2 family molecules in MAB- or AB-induced apoptosis, HepG2 cells were infected with a Bcl-2 overexpressed adenoviral vector. As shown in Figure 4D, overexpression of Bcl-2 effectively reduced the apoptotic cell death induced by MAB and AB, as indicated by increased cell viability and decreased sub-G1 population.

In addition, activation of Fas and Fas ligand (FasL) receptor death pathway has been shown to mediate the induction of apoptosis.<sup>21</sup> We next attempted to determine whether MAB- and AB-induced apoptosis was dependent on Fas/FasL activation. HepG2 cells were treated with 100  $\mu$ M MAB or AB, and expressions of Fas and FasL proteins were determined by Western blot. As shown in Figure 5A, MAB time-dependently increased the levels of Fas and FasL protein expressions. In contrast, AB treatment for 24 h did not affect the Fas and FasL

expression as compared with the negative control (Figure 5A). We then used a Fas antagonist antibody to block the Fas/FasL interaction and test the dependence of the MAB- or AB-induced apoptosis on the Fas-mediated pathway. As shown in Figure 5B, after cotreatment with the Fas antagonist and MAB or AB, the cell viabilities were increased while the sub-G1 populations were diminished.

**MAB and AB Induced Increase in ROS Generation.** Next, we asked whether MAB or AB treatment was associated with changes in intracellular ROS levels. To examine this possibility, cells were loaded with the fluorescent probes DCFDA and HE, which detect hydrogen peroxide ( $H_2O_2$ ) and superoxide ( $O_2^{\cdot-}$ ), respectively, and assessed by flow cytometry in the absence or presence of 100  $\mu$ M of either MAB or AB. Compared with the control group, the generation of intracellular  $H_2O_2$  significantly increased after exposure to each 100  $\mu$ M MAB or AB for 8 h (Figure 6A). The compound MAB effectively increased  $H_2O_2$  generation as early as 1 h and continue up to 8 h as compared with AB. Additionally, the accumulation of superoxide radicals was also detectable from 2 to 8 h after MAB or AB treatment (Figure 6A). To determine whether the pro-oxidant effects of MAB and AB participate in their apoptosis effect, HepG2 cells were pretreated with antioxidant enzymes superoxide dismutase (30 U/mL SOD) and catalase (34 U/mL CAT) and antioxidants *N*-acetylcysteine (1 mM, NAC) and ascorbic acid (0.2 mM, ASC). As expected, the results showed that the presence of the scavenger enzymes (SOD and CAT) and antioxidants (NAC and ASC) abolished the accumulation of intracellular ROS induced by MAB and AB (Figure 6B). Since one of the major sources of ROS generation in cancer cells is NADPH oxidase activation, we then measured the NADPH oxidase activity to address whether it was involved in MAB- and AB-induced oxidative stress in HepG2

cells. Figure 6C shows that MAB and AB could enhance NADPH oxidase activity in HepG2 cells, while this event could be inhibited by DPI, a NADPH oxidase inhibitor. Moreover, treatment with DPI effectively blocked drug-mediated ROS production (Figure 6D) and increased cell viability (Figure 6E), suggesting that NADPH oxidase played a crucial role in MAB- and AB-mediated events. Finally, to further characterize the apoptotic response induced by triterpenoids, the effect of SOD, CAT, NAC, and ASC on the MAB-

and AB-induced cell death was determined by TUNEL assay. The results showed that the presence of the scavenger enzymes and antioxidants significantly attenuated the MAB- and AB-induced apoptotic cell death (Figure 6F). Therefore, the percentage of TUNEL positive cells observed in MAB- and AB-treated HepG2 cells decreased dramatically in the presence of 30 U/mL SOD, 77% vs 50% and 63% vs 51%; 34 U/mL CAT, 77% vs 53% and 63% vs 48%; 1 mM NAC, 77% vs 47% and 63% vs 39%; 0.2 mM ASC,

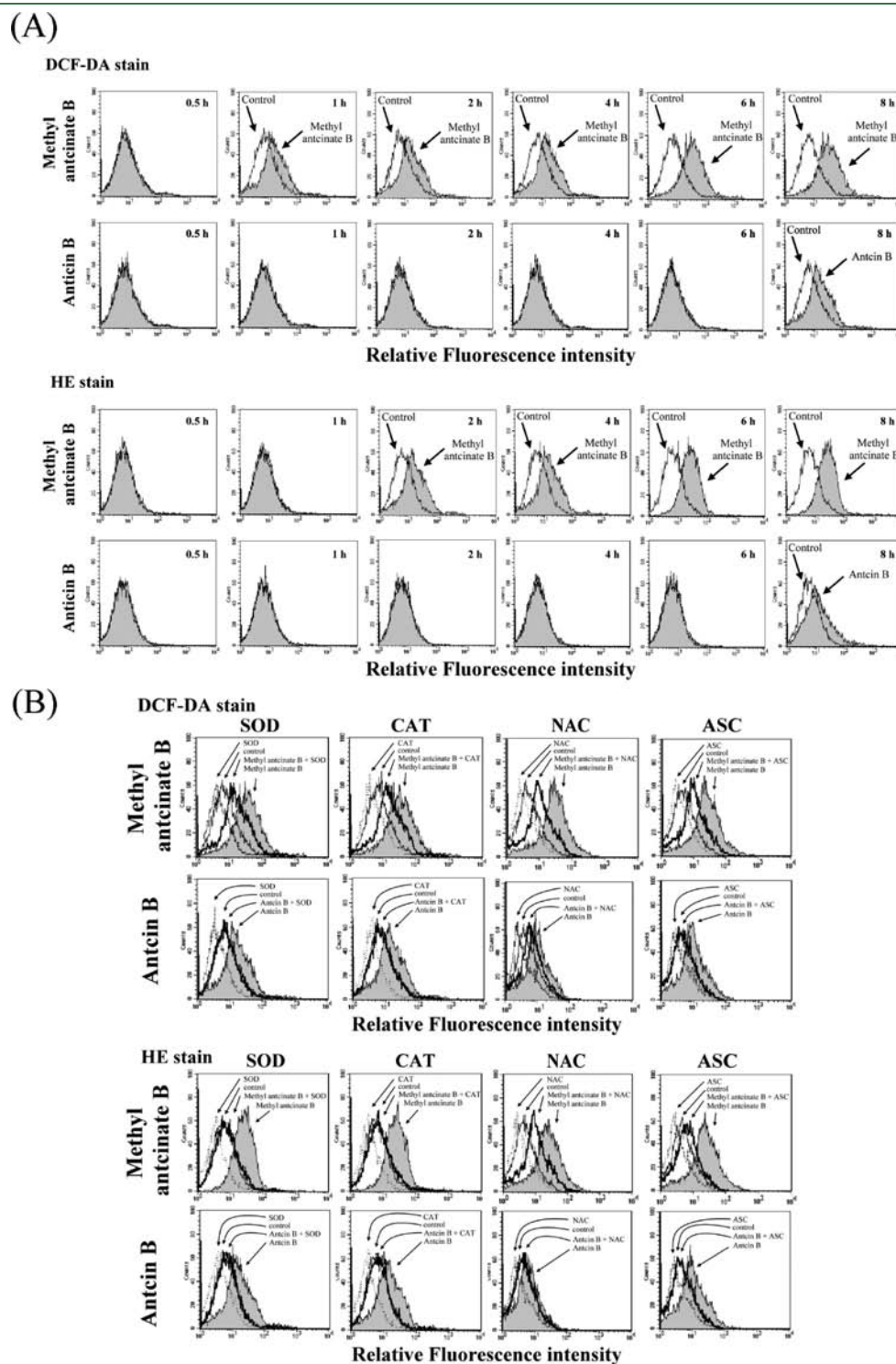
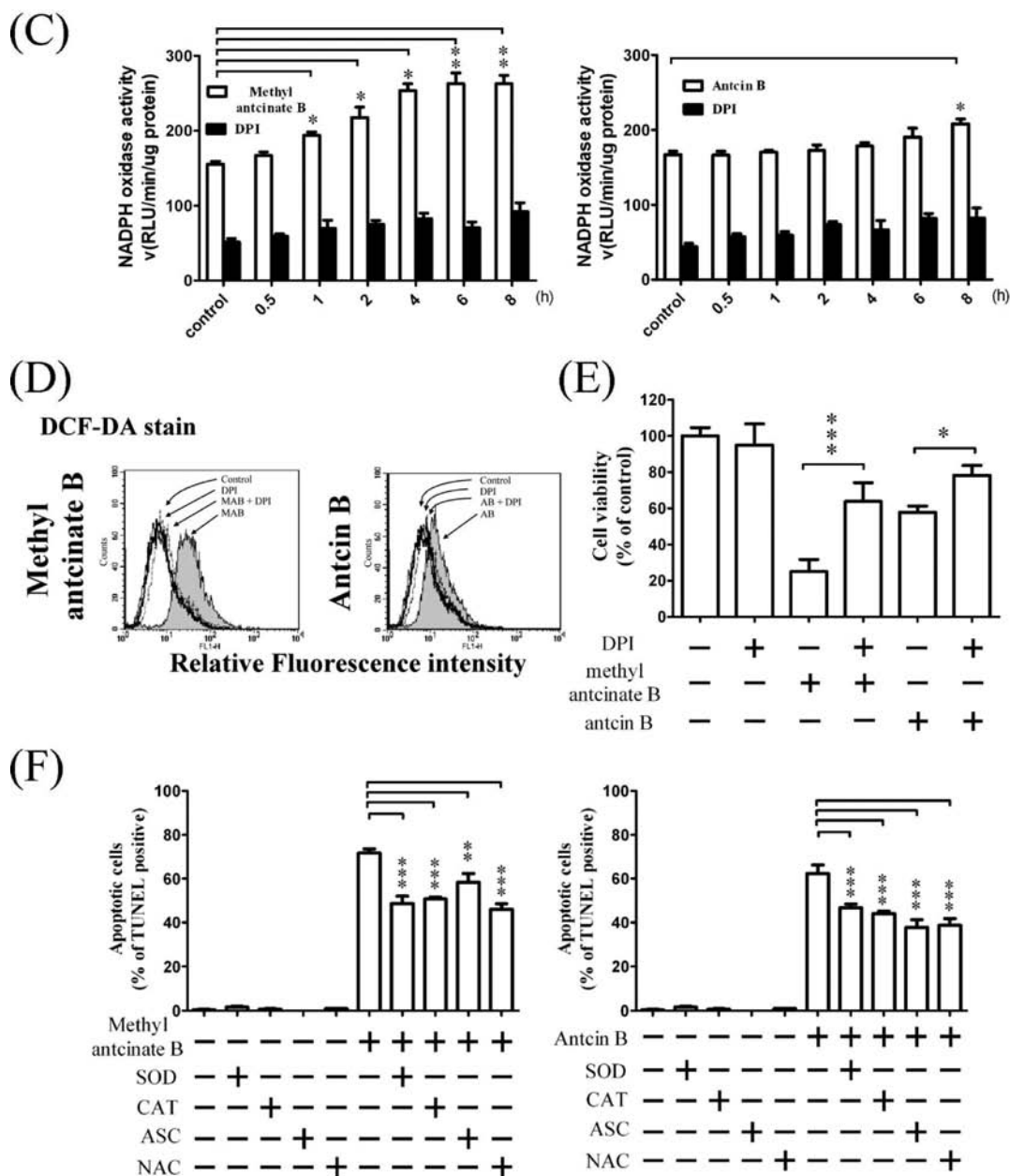


Figure 6. Continued





**Figure 6.** Methylantcin B (MAB) and antcin B (AB) increase ROS production. (A) Cells were treated without or with 100  $\mu$ M MAB or AB for 0.5, 1, 2, 4, 6, and 8 h, the ROS levels were measured by flow cytometry after incubation with DCFDA or HE fluorescence probe stain. (B) Antioxidant enzymes eliminated MAB- and AB-induced ROS generation. Cells were protected by SOD (30 U/mL), CAT (34 U/mL), *N*-acetylcysteine (1 mM NAC), and ascorbic acid (0.2 mM ASC) with 1 h pretreatment when cotreated with 100  $\mu$ M MAB or AB for another 8 h, and the ROS levels were stained with DCFDA. In the graphs, a black line is the control, gray is drug treatment, boldface line is drug with antioxidant, and dotted line is antioxidant only. (C) NADPH oxidase activity assay. Cells were treated with 100  $\mu$ M of MAB for 0.5, 1, 2, 4, 6, and 8 h in the absence or presence of 0.5  $\mu$ M DPI. Reaction velocity ( $v$ ) was calculated as the change in relative light unit (RLU) per minute per microgram of protein. (D) ROS production was determined after 8 h treatment. (E) Viability cells were estimated after 24 h treatment before 2 h exposed with 0.5  $\mu$ M DPI by trypan blue dye exclusion assay. (F) Impact of antioxidant enzymes SOD (30 U/mL) and CAT (34 U/mL) and ROS scavengers ASC (0.2 mM) and NAC (1 mM) on the apoptotic value was determined by TUNEL assay with FACSscan when treated with 100  $\mu$ M MAB or AB media for 24 h. Data are shown as the mean  $\pm$  SD from three independent experiments. The statistic difference level is shown as \* $p$  < 0.05, \*\* $p$  < 0.01, and \*\*\* $p$  < 0.001, as compared to control DMSO treatment values.

77% vs 62% and 63% vs 38%, respectively, confirming the involvement of ROS in the process under study.

## DISCUSSION

HCC is one of the most common types of malignancies that carries poor prognosis worldwide. It is the fifth most common

cancer and the third leading cause of cancer-related deaths, claiming over 1 million lives annually.<sup>22</sup> In Taiwan, HCC is the leading cause of cancer deaths, with approximately 8000 new cases diagnosed and 7000 deaths occurring annually.<sup>23</sup> HCC commonly develop from liver cirrhosis, in which there is continuous hepatocyte regeneration and inflammation; this suggests that DNA damage and ROS are involved in the process of

hepatocarcinogenesis.<sup>22</sup> Although substantial progress has been made in developing chemotherapeutic treatments for HCC, drug efficacy is often outweighed by undesirable side effects.<sup>24</sup> Thus, there is a need to develop new therapies against HCC. In the recent years, phytochemicals and microbial extracts isolated from various sources have shown significant anticancer activities<sup>25–29</sup> and therefore are considered as promising agents for HCC clinical applications.<sup>30</sup> It is estimated that approximately 50% of the drugs currently used in the clinic are derived from the natural products or their synthetic analogs, which still continue to provide essential sources of novel discovery leads. MAB and AB are the components of *A. camphorata*, which has been used historically as a traditional Chinese medicinal mushroom.

First of all, we observed that both MAB and AB were potent inhibitors of HCC cell viability in a dose-dependent manner, the effect of MAB being more pronounced. It has been reported that some anticancer agents cause growth inhibition through interfering with the processes of cell cycle and others cause cell death by apoptosis.<sup>13,14</sup> In our study, apoptotic cell death was determined according to the following four methods. A hallmark of apoptosis in the cells is the generation of DNA fragments, which leads to a characteristic hypodiploid pattern, readily distinguishable by flow cytometry analysis after PI staining.<sup>13</sup> Our results showed that triterpenoids MAB and AB caused DNA fragmentation (Figure 2A). Consistent with generation of DNA fragments, MAB and AB strongly induced PARP cleavage (Figure 2B). In this study, cell cycle analysis revealed a progressive accumulation of cells in the subdiploid phase (sub-G<sub>1</sub>) of the cycle upon exposure to MAB and AB (Figure 2C). This subG<sub>1</sub> is normally associated with apoptosis.<sup>14</sup> The induction of apoptosis by MAB and AB in HepG2 cells was further confirmed by the occurrence of DNA hypoploidy (Figure 2D). Since the DNA fragmentation, PARP cleavage, and cell cycle inhibition have been considered as the key events occurring during apoptotic cell death,<sup>13</sup> we therefore conclude that MAB and AB can kill cancer cells by inducing apoptosis.

Caspases are cytoplasmic aspartate-specific cysteine proteases, and it has been reported that activation of caspase cascade appears to be directly responsible for many agents to induce apoptosis in many types of cancer cells.<sup>20</sup> In particular, activation of caspase-3 plays a central role in the execution of apoptosis. Activation of caspase-3 requires the activation of initiator caspases, such as caspase-8 or caspase-9, in response to pro-apoptotic signals.<sup>20</sup> In this study, HepG2 cells treated with MAB and AB increased the activation of caspase-3, -8, and -9 (Figure 3). It was also observed that reductions of caspase cascades with specific inhibitors could block MAB- and AB-induced apoptosis in HepG2 cells. These factors indicated that MAB- and AB-induced apoptosis was through caspase-dependent responses.

We then conducted a mechanistic study to investigate how MAB and AB activate apoptosis. It is well-known that apoptosis can be activated mainly through two pathways: the death receptor pathway (extrinsic pathway) or the mitochondria-dependent pathway (intrinsic pathway).<sup>14</sup> Both pathways can converge to mitochondria to promote the release of various apoptotic factors, including cytochrome *c*, which can activate downstream targets to trigger cell death.<sup>14</sup> Bcl-2 family proteins are structurally related molecules, which positively or negatively modulate mitochondria-dependent apoptosis.<sup>20</sup> The relative equilibria of various anti- and pro-apoptotic Bcl-2 family members are a critical determinant of cellular homeostasis. The present study supports the involvement of the intrinsic pathway

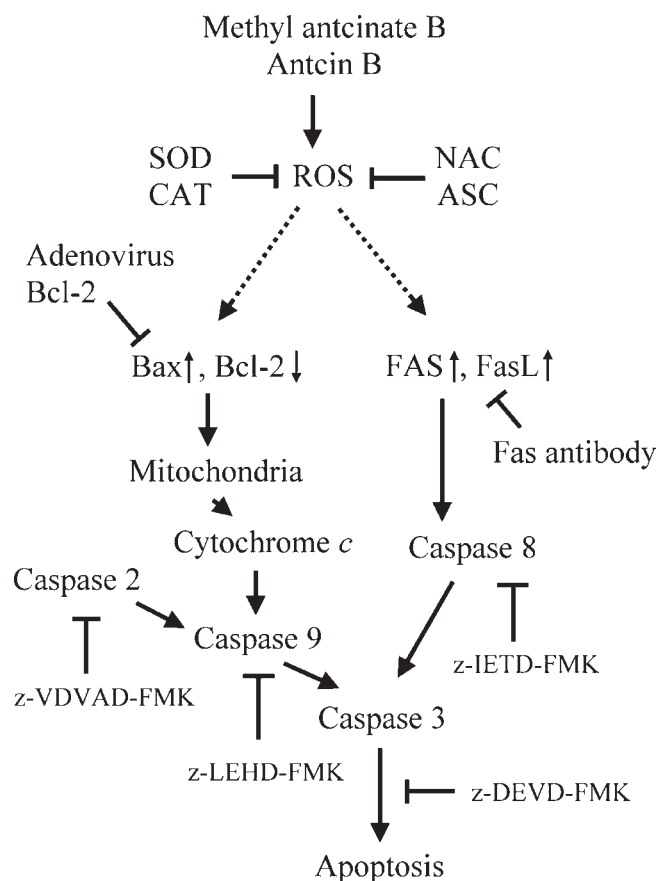


**Figure 7.** Schematic representation of methylantcin B- and antcin B-induced apoptosis in HepG2 cells.

in MAB- and AB-treated HepG2 cells, characterized by Bcl-2 and Bcl-xL down-regulation, Bax up-regulation, and marked disruption of  $\Delta\Psi_m$  (Figure 4). Furthermore, it is known that the transfection of Bcl-2 suppresses drug-induced apoptosis in tumor cells.<sup>31</sup> Our results are in agreement with previous reports that the percentage cell viability increased while sub-G<sub>1</sub> population (Figure 4D) was decreased by MAB and AB in HepG2 cells infected with adenovirus-Bcl-2.<sup>31</sup> Thus, our data demonstrated that the decreased Bcl-2 expression might play an important role in the apoptotic pathway of HepG2 cells induced by MAB and AB. Bax can act on the mitochondria to induce mitochondrial permeability transition, resulting in the release of various components, including cytochrome *c*. This study demonstrated that Bax was translocated to mitochondria, leading to cytochrome *c* release from mitochondria into the cytosol in response to MAB and AB exposure (Figure 4B). Furthermore, our study revealed a time-dependent dissipation of the mitochondrial transmembrane potential, as documented by the loss of the Mito-Tracker Red JC-1 fluorescence as a result of exposure of the cells to MAB and AB (Figure 4C). All these findings indicated that the mitochondria-dependent intrinsic apoptotic pathway was activated by MAB and AB. In anticancer therapy, another key signaling mechanism known to play a role in the execution of apoptosis is the Fas/FasL system.<sup>21</sup> The extrinsic pathway is initiated by death receptors (e.g., Fas, TNFR1) with sequential activation of the initiator caspase-8 and of the effector caspase-3.<sup>21</sup> Our study demonstrated that caspase-3 and -8 were activated, and that both Fas and FasL markers were time-dependently increased in MAB-treated

HepG2 cells, while AB showed only a slight up-regulatory effect (Figure 5A). Furthermore, we found that cocubination of HepG2 cells with MAB or AB and the Fas antagonist antibody increased the cell viability and decreased the sub-G1 population as compared with MAB or AB treatment alone (Figure 5B). Thus, this study demonstrated that the expression of Fas was an important pathway of MAB- and AB-induced apoptosis in HepG2 cells. Taken together, our results suggested that MAB- and AB-induced apoptosis was mediated through both intrinsic and extrinsic pathways.

ROS is generated intracellularly as byproducts of normal aerobic metabolism or as second messengers in various signal transduction pathways or in response to environmental stress.<sup>15</sup> Depending upon the concentration, ROS elicits a wide spectrum of biological responses ranging from mitogenic to proliferative effects at low concentration to macromolecular damage and cell death at high concentrations.<sup>15</sup> The generation of ROS is part of the mechanism by which most chemotherapeutic agents or ionizing radiation kill tumor cells.<sup>32</sup> The rationale behind this idea is that cancer cells are highly dividing ones and they are generally more active than normal cells in terms of ROS production.<sup>32</sup> In addition, it is reported that many tumors have decreased levels or activities of important antioxidant enzymes, including superoxide dismutase-1 and -2 and catalase.<sup>33</sup> This situation makes cancer cells less efficient at removing ROS. They thus are under higher levels of oxidative stress, which can make them more vulnerable to ROS-generating compounds than normal cells.<sup>32</sup> Activation of NADPH oxidase accounts, at least partially, for the increased levels of ROS in several types of cancer.<sup>33</sup> In this study, one of the striking features of the MAB- and AB-induced apoptosis in the HepG2 cells was the accumulation of ROS (Figure 6A). The importance of ROS production in MAB- and AB-treated cells was confirmed by the ability of antioxidant SOD, CAT, NAC, and ASC to inhibit MAB- and AB-induced ROS generation (Figure 6B). In addition, pretreatment with antioxidants rescued HepG2 cells from MAB- and AB-induced apoptosis, indicating that ROS was the up-regulator during these triterpenoids-induced apoptosis. Furthermore, increased activity of NADPH oxidase was observed in MAB- and AB-treated HepG2 cells compared with untreated cultures. Incubation with the NADPH oxidase specific inhibitor DPI significantly suppressed MAB- and AB-induced NADPH oxidase activation (Figure 6C) and ROS production (Figure 6D) and increased cell viability (Figure 6E). These results provide a possible fundamental explanation for why MAB and AB bring about excessive ROS generation in HepG2 cells. Besides, our data also indicate that MAB and AB were potent inducers of oxidative stress, which plays a primary role in triggering the progression of the apoptotic process through activation of both intrinsic and extrinsic pathways in HepG2 cells. In relation to the chemical structures, the triterpenoids MAB and AB can be classified as ester and acid, respectively (Figure 1A). Although the structure–activity relationships of these triterpenoids are far from clear, it seems that the ester group ( $-\text{COOCH}_3$ ) at C-26 in MAB enhanced its cytotoxic capacity as compared to the acidic group ( $-\text{COOH}$ ) at C-26 in AB. These findings shed insights into the diverse caveats of the molecular mechanism of MAB- and AB-induced apoptosis.

In conclusion, this study for the first time showed that the apoptosis induced by *A. camphorata* triterpenoids MAB and AB involves the activation of both intrinsic (mitochondrial) and extrinsic (death receptor) pathways in HepG2 cells. This study

also provides evidence that NADPH oxidase-mediated oxidative stress plays a key role in triggering apoptosis in HepG2 cells. On the basis of the results, a hypothetical diagram depicting a possible mode of apoptotic induction by MAB and AB in HepG2 cells is presented in Figure 7. Thus, there was an opportunity to use MAB and AB as functional food additives or as combinational chemotherapeutic agents along with traditional antihuman liver cancers drugs. However, further studies are needed to examine the in vivo efficacy and pharmacokinetic studies of these triterpenoids.

## ■ ASSOCIATED CONTENT

**S Supporting Information.** The  $^1\text{H}$  NMR,  $^{13}\text{C}$  NMR, and DEPT spectra of methylantcin B (MAB) and antcin B (AB) (Figures S1–S6). This material is available free of charge via the Internet at <http://pubs.acs.org>.

## ■ AUTHOR INFORMATION

### Corresponding Author

\*Y.-M.T.: tel, 886-4-23323000, ext. 4471; fax, 886-4-23395870; e-mail, [ymtzeng@cyut.edu.tw](mailto:ymtzeng@cyut.edu.tw). S.-L.H.: tel, 886-4-23592525, ext. 4039; fax, 886-4-23592705; e-mail, [h2326@vghtc.gov.tw](mailto:h2326@vghtc.gov.tw).

### Funding Sources

This work was supported by National Science Council of Taiwan (NSC 98-2320-B-324-001, NSC 99-2811-M-324-003, and NSC 100-2113-M-324-001-MY3 to Y.-M.T.) and National Science Council of Taiwan (NSC 99-3112-B-075A, and 98HCP005-6 to S.-L.H.).

## ■ REFERENCES

- (1) Ferreira, I. C.; Vaz, J. A.; Vasconcelos, M. H.; Martins, A. Compounds from wild mushrooms with antitumor potential. *Anticancer Agents Med. Chem.* **2010**, *10*, 424–436.
- (2) Geethangili, M.; Tzeng, Y. M. Review of pharmacological effects of *Antrodia camphorata* and its bioactive compounds. *Evidence Based Complementary Altern. Med.* **2011**, Article ID 212641, doi:10.1093/ecam/nep108.
- (3) Wu, M. T.; Tzang, B. S.; Chang, Y. Y.; Chiu, C. H.; Kang, W. Y.; Huang, C. H.; Chen, Y. C. Effects of *Antrodia camphorata* on alcohol clearance and antifibrosis in livers of rats continuously fed alcohol. *J. Agric. Food Chem.* **2011**, *59*, 4248–4254.
- (4) Huang, C. H.; Chang, Y. Y.; Liu, C. W.; Kang, W. Y.; Lin, Y. L.; Chang, H. C.; Chen, Y. C. Fruiting body of *Niuchangchih* (*Antrodia camphorata*) protects livers against chronic alcohol consumption damage. *J. Agric. Food Chem.* **2010**, *58*, 3859–3866.
- (5) Song, T. Y.; Hsu, S. L.; Yen, G. C. Induction of apoptosis in human hepatoma cells by mycelia of *Antrodia camphorata* in submerged culture. *J. Ethnopharmacol.* **2005**, *100*, 158–167.
- (6) Hsu, Y. L.; Kuo, Y. C.; Kuo, P. L.; Ng, L. T.; Kuo, Y. H.; Lin, C. C. Apoptotic effects of extract from *Antrodia camphorata* fruiting bodies in human hepatocellular carcinoma cell lines. *Cancer Lett.* **2005**, *221*, 77–89.
- (7) Song, T. Y.; Hsu, S. L.; Yeh, C. T.; Yen, G. C. Mycelia from *Antrodia camphorata* in submerged culture induce apoptosis of human hepatoma HepG2 cells possibly through regulation of Fas pathway. *J. Agric. Food Chem.* **2005**, *53*, 5559–5564.
- (8) Yeh, C. T.; Rao, Y. K.; Yao, C. J.; Yeh, C. F.; Li, C. H.; Chuang, S. E.; Luong, J. H.; Lai, G. M.; Tzeng, Y. M. Cytotoxic triterpenes from *Antrodia camphorata* and their mode of action in HT-29 human colon cancer cells. *Cancer Lett.* **2009**, *285*, 73–79.
- (9) Rao, Y. K.; Wu, A. T.; Geethangili, M.; Huang, M. T.; Chao, W. J.; Wu, C. H.; Deng, W. P.; Yeh, C. T.; Tzeng, Y. M. Identification of antrocin

from *Antrodia camphorata* as a selective and novel class of small molecule inhibitor of Akt/mTOR signaling in metastatic breast cancer MDA-MB-231 cells. *Chem. Res. Toxicol.* **2011**, *24*, 238–245.

(10) Tsai, W. C.; Rao, Y. K.; Lin, S. S.; Chou, M. Y.; Shen, Y. T.; Wu, C. H.; Geethangili, M.; Yang, C. C.; Tzeng, Y. M. Methylantcinate A induces tumor specific growth inhibition in oral cancer cells via Bax-mediated mitochondrial apoptotic pathway. *Bioorg. Med. Chem. Lett.* **2010**, *20*, 6145–6148.

(11) Hsieh, Y. C.; Rao, Y. K.; Wu, C. C.; Huang, C. Y.; Geethangili, M.; Hsu, S. L.; Tzeng, Y. M. Methyl antcinate A from *Antrodia camphorata* induces apoptosis in human liver cancer cells through oxidant-mediated cofilin- and Bax-triggered mitochondrial pathway. *Chem. Res. Toxicol.* **2010**, *23*, 1256–1267.

(12) Male, K. B.; Rao, Y. K.; Tzeng, Y. M.; Montes, J.; Kamen, A.; Luong, J. H. Probing inhibitory effects of *Antrodia camphorata* isolates using insect cell-based impedance spectroscopy: Inhibition vs chemical structure. *Chem. Res. Toxicol.* **2008**, *21*, 2127–2133.

(13) Indran, I. R.; Tufo, G.; Pervaiz, S.; Brenner, C. Recent advances in apoptosis, mitochondria and drug resistance in cancer cells. *Biochim. Biophys. Acta* **2011**, *1807*, 735–745.

(14) Moffitt, K. L.; Martin, S. L.; Walker, B. From sentencing to execution—The processes of apoptosis. *J. Pharm. Pharmacol.* **2010**, *62*, 547–562.

(15) Liou, G. Y.; Storz, P. Reactive oxygen species in cancer. *Free Radical Res.* **2010**, *44*, 479–496.

(16) Dewaele, M.; Maes, H.; Agostinis, P. ROS-mediated mechanisms of autophagy stimulation and their relevance in cancer therapy. *Autophagy* **2010**, *6*, 838–854.

(17) Shieh, P. C.; Chen, Y. O.; Kuo, D. H.; Chen, F. A.; Tsai, M. L.; Chang, I. S.; Wu, H.; Sang, S.; Ho, C. T.; Pan, M. H. Induction of apoptosis by [8]-shogaol via reactive oxygen species generation, glutathione depletion, and caspase activation in human leukemia cells. *J. Agric. Food Chem.* **2010**, *58*, 3847–3854.

(18) Chen, W. J.; Huang, Y. T.; Wu, M. L.; Huang, T. C.; Ho, C. T.; Pan, M. H. Induction of apoptosis by vitamin D<sub>2</sub>, ergocalciferol, via reactive oxygen species generation, glutathione depletion, and caspase activation in human leukemia cells. *J. Agric. Food Chem.* **2008**, *56*, 2996–3005.

(19) Rao, Y. K.; Fang, S. H.; Tzeng, Y. M. Synthesis and biological evaluation of 3',4',5'-trimethoxychalcone analogues as inhibitors of nitric oxide production and tumor cell proliferation. *Bioorg. Med. Chem.* **2009**, *17*, 7909–7914.

(20) Ola, M. S.; Nawaz, M.; Ahsan, H. Role of Bcl-2 family proteins and caspases in the regulation of apoptosis. *Mol. Cell. Biochem.* **2011**, *351*, 41–58.

(21) Mocellin, S. Targeting death receptors to fight cancer: From biological rationale to clinical implementation. *Curr. Med. Chem.* **2010**, *17*, 2713–2728.

(22) Shaw, J. J.; Shah, S. A. Rising incidence and demographics of hepatocellular carcinoma in the USA: What does it mean? *Expert. Rev. Gastroenterol. Hepatol.* **2011**, *5*, 365–370.

(23) Levin, J. Recent trends in hepatocellular carcinoma (HCC) practice in Taiwan: Report from the global HCC BRIDGE study. 21st Conference of the Asian Pacific Association for the Study of the Liver, Bangkok, Thailand, February 17–20, 2011.

(24) Giglia, J. L.; Antonia, S. J.; Berk, L. B.; Bruno, S.; Dessureault, S.; Finkelstein, S. E. Systemic therapy for advanced hepatocellular carcinoma: Past, present, and future. *Cancer Control* **2010**, *17*, 120–129.

(25) Chidambara Murthy, K. N.; Jayaprakasha, G. K.; Kumar, V.; Rathore, K. S.; Patil, B. S. Citrus limonin and its glucoside inhibit colon adenocarcinoma cell proliferation through apoptosis. *J. Agric. Food Chem.* **2011**, *59*, 2314–2323.

(26) Pan, M. H.; Ho, C. T. Chemopreventive effects of natural dietary compounds on cancer development. *Chem. Soc. Rev.* **2008**, *37*, 2558–2574.

(27) Jayaprakasha, G. K.; Jadegoud, Y.; Nagana Gowda, G. A.; Patil, B. S. Bioactive compounds from sour orange inhibit colon cancer cell proliferation and induce cell cycle arrest. *J. Agric. Food Chem.* **2010**, *58*, 180–186.

(28) Gorlach, S.; Wagner, W.; Podsedek, A.; Sosnowska, D.; Dasty, J.; Koziolekiewicz, M. Polyphenols from evening primrose (*Oenothera paradoxa*)

defatted seeds induce apoptosis in human colon cancer Caco-2 cells. *J. Agric. Food Chem.* **2011**, *59*, 6985–6997.

(29) Patil, B. S.; Jayaprakasha, G. K.; Chidambara Murthy, K. N.; Vikram, A. Bioactive compounds: Historical perspectives, opportunities, and challenges. *J. Agric. Food Chem.* **2009**, *57*, 8142–8160.

(30) Mann, C. D.; Neal, C. P.; Garcea, G.; Manson, M. M.; Dennison, A. R.; Berry, D. P. Phytochemicals as potential chemopreventive and chemotherapeutic agents in hepatocarcinogenesis. *Eur. J. Cancer Prev.* **2009**, *18*, 13–25.

(31) Seitz, S. J.; Schleithoff, E. S.; Koch, A.; Schuster, A.; Teufel, A.; Staib, F.; Stremmel, W.; Melino, G.; Krammer, P. H.; Schilling, T.; Muller, M. Chemotherapy-induced apoptosis in hepatocellular carcinoma involves the p53 family and is mediated via the extrinsic and the intrinsic pathway. *Int. J. Cancer* **2010**, *126*, 2049–2066.

(32) Verrax, J.; Pedrosa, R. C.; Beck, R.; Dejeans, N.; Taper, H.; Calderon, P. B. In situ modulation of oxidative stress: A novel and efficient strategy to kill cancer cells. *Curr. Med. Chem.* **2009**, *16*, 1821–1830.

(33) Kryston, T. B.; Georgiev, A. B.; Pissis, P.; Georgakilas, A. G. Role of oxidative stress and DNA damage in human carcinogenesis. *Mutat. Res.* **2011**, *711*, 193–201.